Department of Electrical
and
Computer Systems Engineering

Technical Report
MECSE-7-2007

Raman optically amplified MSK multi-span transmission systems: simulation

LN Binh, TL Huynh and A. Rahman

MONASH
UNIVERSITY

Raman optically amplified MSK multi-span transmission systems: simulation

L.N. Binh, T.L. Huynh and A. Rahman
Center for telecommunications and Information Engineering,
Department of Electrical and Computer Systems Engineering,
Monash University, Clayton Victoria 3168 Australia
Email: le.nguyen.binh@eng.monsh.edu.au
Tel. +613 99053475 fax +613 99053454

Summary

Distributed Raman amplification has emerged as a most attractive amplification scheme in recent research on 40-Gb/s wavelength-division multiplexing (WDM) transmission with merits of uniform gain profile and up to 13-THz dynamic operation bandwidth. However, to the best of our knowledge, there are few works that report numerical comparisons between different pumping schemes in long haul optical transmission systems, especially when the minimum shift keying (MSK) modulation is employed. This paper thus investigates the performance and compatibility of Raman optical amplification (ROA) with linear MSK modulation format for transmission of signals of 40 Gb/s optical DWDM systems. Employing NZ-DSF and dispersion compensated fibre (DCF), we investigate the optical distributed amplification with five Raman pumping configurations namely backward, forward, bidirectional, reverse bidirectional pumping and mid-span bidirectional pumping. Both pure Raman and/or hybrid discrete and distributed Raman/EDFA amplifications have been investigated in order to enhance the quality of transmitted and the transmission performance is compared with lumped optically amplified systems.

Different Raman pumping schemes are numerically simulated using MATLAB for 40 Gb/s single channel, the pump depletion is not taken into account. The power and gain distribution along fibres is incorporated in each step of the non-linear Schroedinger propagation equation (NLSE) and solved numerically using the Split-Step Fourier algorithm. A SIMULINK model is developed for simulation of MSK optically amplified transmission system under differently configured Raman amplification. System performance has been compared with EDFA system under different multi-span configurations. Operational parameters such as input signal power, number of spans and distance of mismatched dispersion compensated fibre are used. The pumping configuration characteristics and optimum span lengths for the systems are presented.

The followings are achieved: (i) A BER of better than 10^{-11} is achieved over a propagation distance of 540km with EDFA amplification and fully dispersion compensated fibre multi-span; (ii) A BER of better than 10^{-10} is achieved over propagation distance of 720km with bi-directional Raman amplification and fully dispersion compensated fibre multi-span;(iii) A propagation length of 1080km can be integrated into system with 0.1mw signal power using Mid-span and Bi-directional Raman pump configuration; (iv) A propagation length of 1440km can be integrated into system with 0.1mW signal power using backward Raman configuration; and (v) A propagation length of 360km can be integrated into system with 0.1mW signal power using Forward Raman configuration.

CONTENTS

TABLE OF FIGURES

1 Introduction

Over the past decades, the transmission reach of optical fiber networks has increased significantly. This increase has been made possible by employing optical amplifiers and more recently the employment of different modulation techniques including phase, frequency modulation of the lightwave carriers in the photonic domain. Optical amplifiers are naturally employed. Both discrete and distributed amplification ca be used. Distributed Raman amplification (DRA) can be considered for long-haul and ultra long-haul fiber-optic transmission systems, especially under the condition that expansion of the non-repeater span is required.

The transmission distance is impeded by fiber loss and dispersion. Traditional methods to overcome such limitation are electrical conversion of the optical signal, such as repeaters. These repeaters retransmit signals at progressive stages are becoming increasingly complex and expensive. Raman amplifier upgrades communication medium to a repeater-less transmission fiber, where optical gain is distributed and can be adapted by adjusting the pump wavelengths, thus compensating the fibre loss. Ever increasing capacity requirement for communication network has not only generated the need to develop optical amplifiers but also novel modulation format to provide better exemption to mutilation arising from amplified spontaneous noise, dispersion and fiber nonlinearity effects, as well as the spectral efficiency.

Much work has been carried out on on-off keying (OOK) signal, differential quadrature (DQPSK) and even continuous phase frequency shift keying (CPFSK) recently [12]. Advanced modulation format s such as return to zero (RZ-DPSK) and carrier suppressed CSRZ-DPSK has shown promising performance in long haul transmission. Comparing with CSRZ-DPSK or RZ-DPSK, minimum shift keying (MSK) offers additional advantages against large dispersion tolerance, more robust against Inter-symbol Interference (ISI) and minimum noise contribution if frequency discrimination is used at the receiver. Furthermore, MSK signal exhibits constant amplitude and continuous phase at every bit transition time and lower side lobes. Its main lobe of the power spectrum is narrower than that of the QPSK and DPSK .In addition the side lobes in MSK is much more suppressed, making it easier to be filtered. Higher signal energy contains in the main lobe of MSK spectrum. These features make MSK a preferable data modulation format for high speed and high spectral efficiency system. As a result, MSK can be considered s a potential modulation format for long-haul communications incorporating Raman amplification.

This paper describes the transmission simulation of an optically amplified transmission system using Raman amplification with 40 Gb/s Minimum Shift Keying (MSK) modulation scheme. Different processes and steps are triumphed over to complete the projects. Firstly, numerical techniques are studied and modified in the MATLAB programming landscape to solve various Raman pump configurations for a single channel system Such configurations are backward, forward, bi-directional and reverse bi-directional. The signal wavelength is operating in the C-band (1525-1565nm) range at 1550nm. Raman amplification has been launched into the single fibre mode with pump wavelength of 1450nm. This is because the Raman amplification performs its best at 100nm difference between signal and pump wavelength. Secondly, various Raman pumping configurations are used for the study of the evolution of a single Gaussian pulse operating at 40Gb/s through a fiber span length using the Split-Step Fourier Method (SSFM). Finally, the numerical analysis of Raman pump configurations are integrated to a Simulink optical modulation format such as Minimum-Shift Keying (MSK) and compare the performance against EDFA, by means of control parameters such as number of spans, input peak power, SMF length fully compensated fibre and mismatched compensation using DCF etc.

MSK optical transmitters may consist of two dual-drive $LiNbO_3$ Mach-Zehnder interferometer modulators (MZIM) generating I and Q components of MSK modulated signals. The upper and lower arms of the dual-drive MZIM modulator are biased at $V_{\pi/2}$ and $-V_{\pi/2}$ respectively and driven with data and complemented data sequences. Phase shaping driving employs periodic triangular wave sources for linear MSK generation. A non-coherent configuration for differential detection scheme is used at the receiver for the detection of optical MSK sequences. The receiver consists of an integrated optic one-bit phase comparator, the Mach-Zehnder Delay Interferometer (MZDI), and balanced photodetector pair [20]. An additional $\pi/2$ phase shift is introduced to detect the differential $\pi/2$ phase shift difference of two adjacent optical MSK pulses of the I- and Q-channels.

The paper is organised as follows: a simple background of optical fibre dispersion and nonlinearity is given in Section 2 as well as the fundamental aspects of Raman amplification and its operation. Single and dual drive MZIM

are given in Section 3. In Section 4, the performance of a system is discussed including the interpretation of eye diagram, the Bit error rate (BER) and probability distribution. Section 5 outlines the principles of MSK modulation format and its implementation in MATLAB SIMULINK. SIMULINK model of the optical transmitter, optical modulator, fiber propagation and balance receiver are discussed in Section 6. Section 7 focuses on different Raman pump configurations and their distributed gain. The accuracy of each pump configuration is also proven using a single Gaussian pulse prior to the transmission over a multi-span optically amplified system. In Section 8, the bit error rate (BER) obtained for EDFA multi-span transmission and various Raman pump arrangements are analyzed.

2 Optical fiber as a transmission and gain medium

2.1 Dispersion and attenuation

The frequency dependence of the group velocity leads to pulse broadening simply because different spectral components of pulse delay after the propagation. The dispersion factor is given as

$$D = -\frac{2\pi c}{\lambda^2}\beta_2 \tag{1}$$

where β_2 is the GVD parameter; at 1.55μm wavelength region**.** As optical receivers need a certain minimum amount of power for recovering the signal accurately, the transmission distance is essentially limited by fiber losses. So, the longer the fibre length, the more power of the signal will be lost. Attenuation is measured by total power loss per unit length of fibre. If *P*in is the power launched at the input end of a fibre of length *L*, the output power P_{out} is given by

$$P_{out}(t) = P_{in}\exp(-\alpha L) \tag{2}$$

where α is the attenuation coefficient. Fibre losses depend on the wavelength of transmitted light. Both standard SMF and Non-Zero Dispersion Shifted fibre (NZ-DSF) can also be used.

2.2 Nonlinear Effects

The response of any dielectric to light becomes nonlinear for intense electromagnetic fields, and optical fibres are no exception. Even though silica is intrinsically not a highly nonlinear material, the waveguide geometry that confines light to a small cross section over long fibre lengths makes nonlinear effects quite important in the design of modern light wave systems[1]. At high power levels, the nonlinear phenomena of stimulated Raman scattering (SRS) and stimulated Brillouin scattering (SBS) become important. The intensity of the scattered light in both cases grows exponentially once the incident power exceeds a threshold value. These inelastic scattering systems are scattering in which the frequency of the light is shifted downwards. The differences between the two in single mode fibres are that SBS occurs in backward direction and SRS occurs bi-directionally [11].

SRS occurs in optical fibre when pump wave is scattering by a silica molecules. Some pump photon gives up their energy to create other photon of low energy at a lower frequency which absorbed by silica molecules. Another major contribution to non linear effect is nonlinear phase modulation. All material behaves nonlinearly at a high intensity and their refractive index changes or increase with intensity. Therefore propagation constant becomes power dependent [15]. SPM (self phase modulation) is a self-induced phase shift experienced by an optical field during its propagation in an optical fiber under intense power

$$\phi_{NL} = \bar{\gamma} P_{in} L_{eff} \tag{3}$$

ϕ_{NL} is the phase shift cause by nonlinearity where nonlinearity co-efficient is represented as $\bar{\gamma} \approx 2W^{-1}km^{-1}$. The SPM induced spectral broadening is a consequence of the time dependence of ϕ_{NL} : a time-dependent phase shift according to the time-dependent pulse intensity. In this way, an initial un-chirped optical pulse acquires a so-called chirp, i.e. a temporally varying instantaneous frequency [2]. In the frequency domain, strong self-phase modulation can lead to a spectrum with strong oscillations. The reason for this is basically that the instantaneous frequency undergoes strong excursions, so that in general there are contributions from two different times to the Fourier integral for a given frequency component..

2.3 Raman amplification

2.3.1 Stimulated Raman Scattering (SRS)

For generation of the SRS, a large pump wave (usually less than 500mW) is co-launched into the fibre at a lower frequency to that of the lightwave signal to be amplified [2] .The Raman gain depends upon the pump power and the frequency offset between pump source and the information carrier-modulated signals. Amplification occurs when the lower frequency pumping photons transfers their energy to new higher frequency photons at the signal wavelength. Raman amplification occurs in the transmission fiber. However, the selection of pump powers and wavelengths, as well as the number and separation of pumps, strongly determines the wavelength dependence of Raman gain and noises [17]. SRS is a nonlinear effect due to interactions between light waves with molecular vibrations in silica fibre. For a single channel the threshold of the required pump power is:

$$P_{th} = \frac{16A_{eff}}{K_P L_{eff} g_r} \tag{4}$$

where K_p is the polarisation constant ≈ 2. Scattering occurs when the polarization of the molecule changes with the vibration motion [1].

2.3.2 Raman gain

There is a wide range of transitions providing Raman gain in the vibrational state. The gain flatness of about l00nm (~13THz) shift from the original pump signal can be achieved. The usable gain bandwidth is approximately 48nm. To obtain maximum gain on a particular wavelength, multi-wavelength pump sources can be used[17].

The overall optical gain can be expressed in terms of the pump intensity or power, I_p or P_p as

$$g(\nu) = g_R(\nu) I_P = g_R(\nu) \frac{P_P}{A_{eff}} \tag{5}$$

This shows that the gain is dependent upon the frequency and pump power [1].The Raman gain efficiency, $g_{R\_eff} = g_R / A_{eff}$ is a critical design issue, in terms of comparison between different fibres in the system. Different fibres have different gain efficiencies due to smaller effective areas and different Ge:doped concentrations which would alter the overall Raman gain efficiency and hence optical gain.

2.3.3 Amplification coupled Equations

When a weak signal is launched with a stronger pump, it will be amplified due to SRS. In the CW case, the signal amplification is described by the two coupled equations in terms of power transfer along a length of a fibre (z) from the pump to the signal due to the Raman interaction between the pump and the signal:

$$\begin{aligned} \frac{dP_s}{dz} &= -\alpha_s P_s + \frac{g_R}{A_{eff}} P_P P_s \\ \frac{dP_P}{dz} &= -\alpha_P P_P + \frac{\nu_P}{\nu_s} \frac{g_R}{A_{eff}} P_P P_s \end{aligned} \tag{6}$$

It illustrates that the pump power provides the energy for amplification and depletes as signal power increases. As pump signal transfer all the energy to the signal power, the optical gain is reduced and gain saturation occurs [2]. The power along the length of the fiber is also reduced by the fiber losses, which occur in the medium due to its intrinsic properties. It is also a limiting factor in transmission distance lengths as optical receivers require minimum amounts of power to recover the signal [22]. The attenuation co-efficient, $\alpha_{P,S}$ includes all sources of power attenuation. The backward pumping case can be considered into similar fashion however using boundary condition, $P_p(L) = P_0$, the pump power becomes:

$$P_P(z) = P_0 \exp[-\alpha_p(L-z)] \tag{7}$$

Similar expression of the pump power long the propagation length can be obtained for the case of forward pumping. Bidirectional pumping is slightly more complicated because two pump laser are located at the opposite fibre end in most configuration. The pump power becomes:

$$P_P(z) = P_0\{r_f \exp(-\alpha_p z) + (1+r_f)\exp[-\alpha_p(L-z)]\} \tag{8}$$

where r_f is the percentage of power launched in forward direction as it varies from 0 to 1. The signal intensity at amplifier output at length L is determined as:

$$P_P(z) = P_S(0)e^{[\frac{g_R P_0 L_{eff}}{A_{eff}} - \alpha_S L]} \tag{9}$$

where L_{eff} is the effective length; at this point where nonlinearity take place and it is defined as:

$$L_{eff} = \frac{1 - e^{e^{-\alpha_P L}}}{\alpha_P} \tag{10}$$

It is usually required to set the overall net signal gain such that $G(z) = 1$; to compensate the fibre loss and in order to find out required total pump power [22]. The net signal gain is expressed as:

$$G(z) = \frac{P_S(z)}{P_S(0)} = \exp(g_R \int_0^Z P_P(z)dz - \alpha_S z) \tag{11}$$

Gain amplification contributed by Raman amplifier is the ratio of the power of the signal with and without Raman amplification is given by:

$$G_A = e^{g_0 L} \tag{12}$$

where the small signal gain, g_o, is defined as:

$$g_0 \simeq \frac{g_R P_0}{A_{eff}\alpha_P L} \tag{13}$$

2.3.4 Raman amplification noise

The phenomenon that limits the performance of distributed Raman amplifiers most turns out to be Rayleigh scattering. Rayleigh scattering occurs in all fibres and is the fundamental loss mechanism for them. A small part of light is always backscattered because of this fact. Normally, this Rayleigh backscattering is negligible. However, it can be amplified over long lengths in fibres with distributed gain and affects the system performance in two ways. First, a part of backward propagating noise appears in the forward direction, enhancing the overall noise. Second, double Rayleigh scattering of the signal creates a crosstalk component in the forward direction. It is this Rayleigh crosstalk, amplified by the distributed Raman gain that becomes the major source of power penalty. [2]

Raman amplifiers can work at any wavelength as long as the pump wavelength is suitably chosen. This property, coupled with their wide bandwidth, makes Raman amplifiers quite suitable for WDM systems. An undesirable feature is that the Raman gain is somewhat polarization sensitive. In general, the gain is high when the signal and pump are polarized along the same direction but is reduced when they are orthogonally polarized. The polarization problem can be solved by pumping a Raman amplifier with two orthogonally polarized lasers.

3 Optical Modulators and MSK modulation formats

An optical modulator is a device which allows manipulating a property of light – often of an optical beam, e.g. a laser beam. Depending on which property of light is controlled, modulator can turn into intensity modulators, phase modulators, polarization modulators, etc.[15]. External modulation is preferred than direct modulation as direct modulated laser source suffer from large shifts in the optical carrier frequency, also known as chirp. Generally, external modulators consist of electro absorption modulators and electro-optic modulators. In 10 Gb/s or 40 Gb/s

DWDM applications, electro optic modulators are the technology of choice due to better performance in terms of chirp and modulation speed compared to electro absorption devices.[3]

Mach-Zehnder intensity modulators (MZIM) are used to convert the binary data to be transmitted from the electrical to the optical domain. The output is the phasor sum of two lightwaves that travel through two different paths of the potential different optical path length. The phasor sum can be constructive or destructive, depending on the relative phase of the light waves of the two different paths. If the light waves from two arms are in phase, "ON" state of logic 1 is inferred due to constructive interference. The output is interpreted as "OFF" state or logic 0 if the light waves are π (or 180 degree) out of phase derived from destructive interference [6].

A phase modulator is normally an integrated electro–optic device, LiNbO3, in which the Ti:diffused waveguide is placed in the middle of a travelling wave electrode structure. The electro–optic effect generates the change of the refractive index under the influence of an applied electric field. The input signal is of E_i and it is split into two equal electric fields of $E_i/2$ each. The combined signal at the other end of the Y-junction is given by the equation. Positive and negative electric field changes the index in opposite direction.

$$E_o = \frac{E_i}{2}\left[1+\exp\left(j\pi\frac{V(t)}{V_\pi}\right)\right] = E_i\cos\left[\frac{\pi}{2}\frac{V(t)}{V_\pi}\right]\exp\left[j\frac{\pi}{2}\frac{V(t)}{V_\pi}\right] \tag{14}$$

Therefore the relationship input and output electric field is

$$\frac{|E_o|^2}{|E_i|^2} = \cos^2\left[\frac{\pi}{2}\frac{V(t)}{V_\pi}\right] \tag{15}$$

Depending on the biasing point on the intensity curve, the modulator would have different chirp parameter. Positive chirp corresponds to biasing at the positive slope of the curve, whereas negative chirp corresponds to biasing at the negative slope of the curve.

A dual drive MZIM can be used to reduce the driving voltage, especially when the driving speed is in the GHz range, by driving both arms of the optical waveguides of the MZ structure in a push-pull manner. Thus the intensity modulation cn be implemented by placing a phase modulator in both arms of the interferometer. The effective phase modulation can be increase by using push and pull configuration in driving the interferometer. Phase modulators are driven with modulation voltages of opposite polarities. As a consequence, dual drive MZIM has an attractive feature; it can be driven as phase modulator and intensity modulator by changing its driving voltage [3]

For the input-output relationship of dual drive MZIM is

$$E_o = \frac{E_i}{2}\left[\exp\left(-j\pi\frac{V(t)}{2V_\pi}\right)+\exp\left(j\pi\frac{V(t)}{2V_\pi}\right)\right] = E_i\cos\left[\frac{\pi}{2}\frac{V(t)}{V_\pi}\right] \tag{16}$$

where Vπ is reduced by half due to the opposite phases of $\pm\frac{\pi V(t)}{2V_\pi}$. $\frac{\pi V(t)}{V_\pi}$ is the differential phase shift between the two arms of the modulator.

4 System performance

The role of an optical receiver is to convert the optical signal back into electrical form and recover the data transmitted through the light wave system. Its main component is a photo-detector that converts light into electricity through the photoelectric effect.

Continuous random variables (like voltage or current) have the probability that their value lies within the interval (x… x+dx), according to their probability density function. A very common distribution of the probability density function is the Gaussian distribution:

$$\varphi(\lambda) = \frac{1}{\sigma\sqrt{2\pi}}\cdot e^{\frac{\lambda^2}{2}} \tag{17}$$

Where $\lambda = \frac{x-\mu}{\sigma}$; $\varphi(\lambda) =$ Probability density function; μ is the mean Value ; and σ is the standard deviation .

The integral of the Gaussian distribution gives the probability that x is smaller than a certain threshold x_0, following an error function:

$$\Phi(\lambda) = erf(\lambda) = \int_{-\infty}^{\lambda} \varphi(t)dt \tag{18}$$

As this integral can only be solved by approximation. The probability that the sample is within a certain interval is: ± 1σ =68.27%; ± 2σ = 95.45%; ± 3σ =99.73%. The Q factor measures the quality of a digital transmission signal in terms of its signal-to-noise ratio (SNR). As such, it takes into account physical impairments to the signal (e.g., noise, chromatic dispersion, and any polarization or nonlinear effects) which can degrade the signal and ultimately cause bit errors. In other words, the higher the value of Q factor the better the SNR and therefore the lower the probability of bit errors.

Specifically, Q factor represents the quality of the SNR in the eye of a digital signal, the "eye" being the human eye-shaped pattern on an oscilloscope that indicates transmission system performance. The best place for determining whether a given bit is a 1 or a 0 is the sampling phase with the largest eye opening. The larger the eye opening, the greater the difference between the mean values of the signal levels for a 1 and a 0. The greater that difference, the higher the Q factor and the better the BER performance would be.

The mathematical expression about the relationship between noise, the signal levels and the decision level V_D and bit error rate is:

$$BER = \frac{1}{4}\left[erfc\left(\frac{V_1 - V_D}{\sigma_1\sqrt{2}}\right) + erfc\left(\frac{V_D - V_0}{\sigma_0\sqrt{2}}\right)\right] \tag{19}$$

which can be simplified in term of a Q factor as:

$$BER = \frac{\exp(-Q^2/2)}{Q\times\sqrt{2\pi}} = 0.5erfc(\frac{Q}{\sqrt{2}}) \tag{20}$$

where $Q = \frac{(V_1 - V_0)}{\sigma_1 + \sigma_0}$ and V_D =decision threshold.

5 MSK modulation scheme and transmission

The main principles of the generation of MSK are (i) Depending on the binary data, the phase of signal changes; data 1 increases the phase by π/2, while data 0 decreases the phase by π/2. (ii) A two dimensional signal modulator .Not because it sends two bits per symbol, but it uses two independent orthogonal signal (a sine and cosine) to create the symbol.(iii) MSK signal consists of I- and Q- components. A phase modulation signal can be seen as a combination of two orthogonal signals; (iv) Even and Odd bits are fetched into the I- and the Q- channel respectively over a double bit period (v) the I-component consists of half-cycle cosine wave and Q- bit of half sine; (vi) During even bit interval, the I- component consists of positive cosine waveform for phase of 0, while negative cosine waveform for phase of π; during odd bit interval, likewise the Q-component consists of positive sine waveform for phase of π/2, while negative sine waveform for phase of –π/2; (vii) Only state 0 or π can occur during any even bit interval and only π/2 or –π/2 can occur during any odd bit interval.(viii) The I- and Q-components are delayed by 1 bit period with respect to each other. This is to avoid the phase transition involving 180 degree shift, since phase can not change within two channels at the same time. (ix) In MSK, the sinusoid weight function of each channel passes through zero crossing at the start and the end of the channel. (x) The transmitted signal is the sum of the I- and Q- components. The shape is continuous changing, so there is no disconnected jump in modulation signal at the edge of the symbol.

The state diagram for MSK signal modulation is shown in Figure 1.

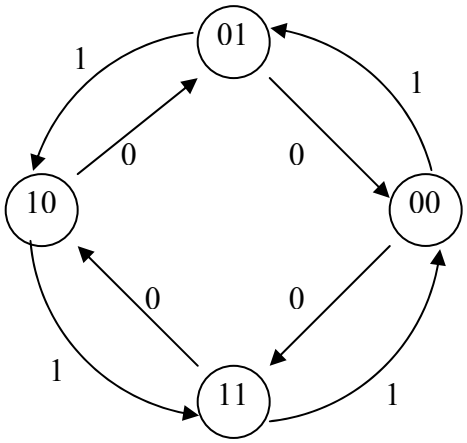

Figure 1: State diagram of the optical carrier for generation of MSK signals

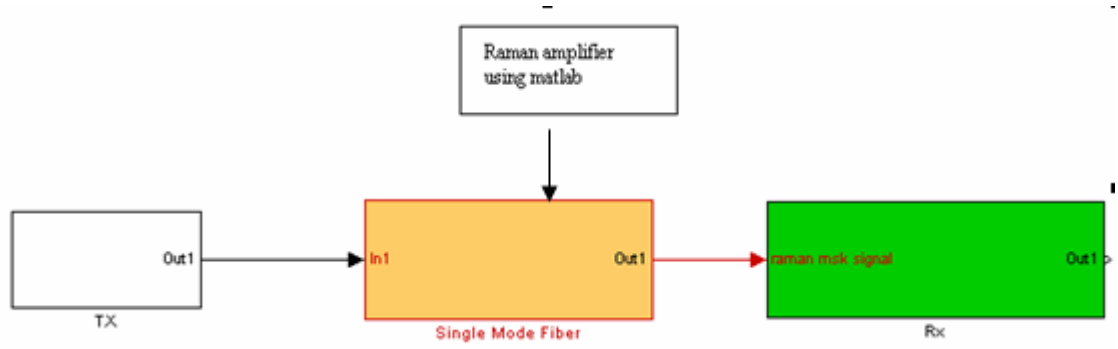

Figure 2 Simulink model for MSK with ROA

An optical communications link comprises an optical transmitter including a single-longitudinal laser and an external electro-optic modulator, transmission medium which is a length of fibre, and a high speed receiver at the other end. An electrical signal is used to modulate the external modulator, and an optical detector in the receiver produces a faint electrical output which is electrically amplified and then demodulated to extract the signal. The gain of an optical amplifier, i.e. the ratio of photons emitted per photons received (the ratio of output optical power to input optical power), is dependent upon the length of the amplifier and the gain per unit length of the excited medium.

5.1 MSK optical transmitter model

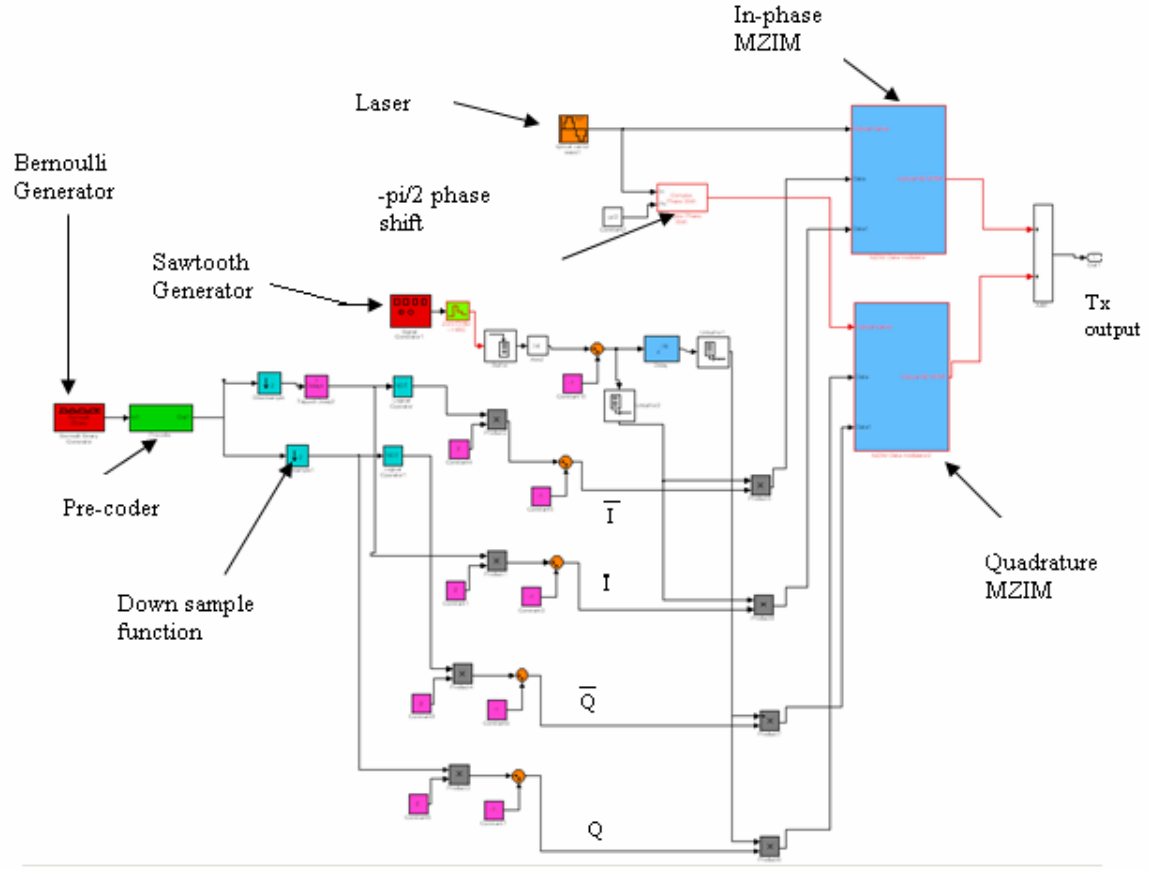

Figure 3 MSK transmitter Matlab Simulink model.

A Bernoulli binary generator block generates streams of random binary bits of 1 and 0 at the rate of 40Gbits/s. A probability of 0.5 is set to be generated (bit 1 and 0) consecutively. The transmitter consists of Bernoulli binary generator, precoder, splitter and two MZIMs. The precoder pre-processed the binary bits to produce serial stream of MSK binary data. MSK binary data follows the state diagram. The splitter divides the bit stream into I and Q channel which then fetched to MZIMs. One MZIM correspond to I channel furthermore second MZIM correspond to Q channel. The outputs of these two MZIM then are added to produce optical MSK signal.

5.1.1 Pre-coder

Conventional I and Q-type receivers for MSK-type modulations suffer a small performance penalty due to the inbuilt deferential encoding operation performed at the transmitter and the attendant requirement for deferential decoding at the receiver. A simple fix to this problem is to pre-code the input data with a deferential decoder which in effect cancels the deferential encoding operation at the transmitter and eliminates the need for deferential decoding at the receiver. From a spectral standpoint, this precoding operation has no effect on the power spectral density of the transmitted signal when the input data are balanced. However, when the input data are unbalanced, the precoder has a definite effect on the transmitted signal the power spectral density.

The detected bit sequence at the receiver output is not equal to the bit sequence at the transmitter input. However, bit sequence at the receiver output is a function of bit sequence at the transmitter input [4] as shown in Figure 4.

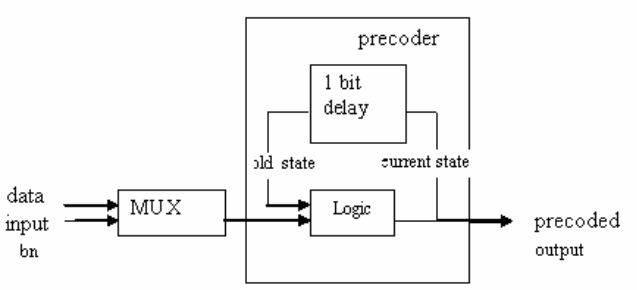

Figure 4: Pre-coder logic circuit

The current state is 1-bit delayed and fetched into logic block as old state. Because the old state needs to be stored in the memory since its binary data indicates the state of the current signal.

5.1.2 Splitter

The output of precoder is fetched into the splitter which separates the serial bit sequence into two parallel bit streams: I- component containing even bit interval output and the quadrature (Q) component containing odd bit interval output. Hence a down sample function has been implemented for I and Q channels with a factor of 2. For the I-channel, the sample offset is none thus the sampling starts from 0, whereas the Q-channel has sample offset of 1 bit. Such parameters causes I channel to sample even bits (0..2..4…2n) and Q-channel to sample odd bits (1..3..5..(2n+1)).etc.

The I-channel with the even bit sequence experiences a 1-bit delay by a parameter tapped delay line. Both I- and Q- components are afterwards separated into two complementary paths. This is to drive the electrodes of the I- and Q- of a dual MZIM, as the I- or Q- driving bits has to be complemented to maintain push pull operation. Therefore, four driven signal are created and they are multiplied by constant 2 so the bit period is twice the data bit period. In phase output is pulse shaped with the triangular pulse shaping waveform with two bit period, whereas Q- output is pulse shaped with one bit period delayed triangular pulse shaping waveform with respect to the I- path. Hence they are interleaved with each other as shown in Figure 5.

5.1.3 MZIM Data Modulator

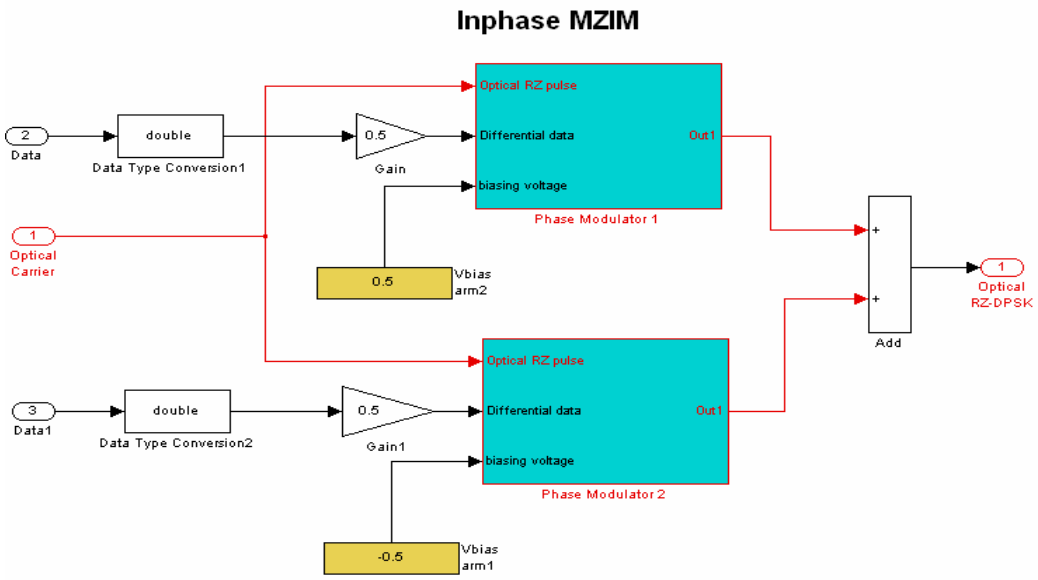

Figure 5: I- data modulator structure using Matlab Simulink model.

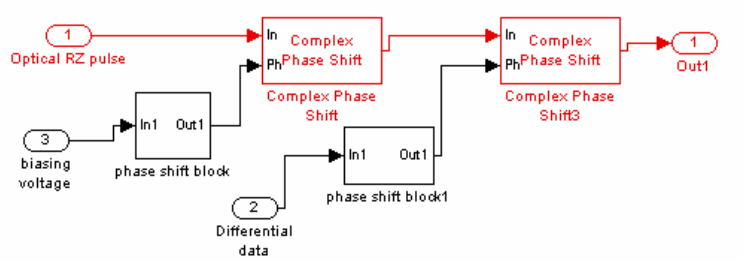

Figure 6: Phase modulation in one arm of the dual drive MZIM.

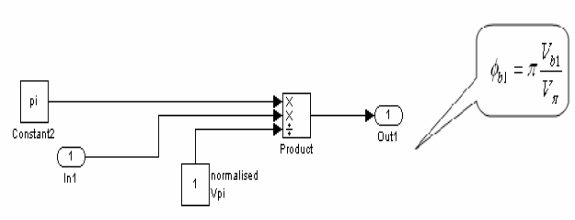

Figure 7: Phase shift bock component

Two dual-drive MZIM data modulators are used for the implementation of the transmitter, one for the I-component and the other for Q-channel. Driven signals which are produced by the splitter and the bias voltage are set to be complemented o each other so they can be applied in upper and lower arm of the phase modulated waveguides in a push pull manner. In other words, opposite polarity are sets such that the two arms have a phase difference of π. Both the I and Q MZIMs are driven with a bias voltage of $0.5V_\pi$ and $-0.5V_\pi$. In a dual drive MZIM upper arm experiences a phase shift induced by the bias voltage and a phase shift due to the driven voltage or signal. Similarly, lower arm will also be influenced by phase shift due to the bias and driven signal. The electric field of the upper arm is thus given by

$$E_u = \frac{E_i}{2}\cos\left[\omega_c t + \phi_{b1} + \phi_{d1}\right] \tag{21}$$

where $\phi_{b1} = \pi \frac{V_{b1}}{V_\pi}$, ϕ_{b1} =phase shift due to bias voltage , V_{b1} = bias voltage . Similarly the electric field for lower arm is given by

$$E_l = \frac{E_i}{2}\cos\left[\omega_c t - \phi_{b2} - \phi_{d2}\right] \tag{22}$$

where $\phi_{b2} = \pi \frac{V_{b2}}{V_\pi}$, ϕ_{b2} = phase shift due to bias voltage. Thus the out put of the I-channel MZIM is

$$E_o = \frac{E_i}{2}\cos\left[2\omega_c t + \phi_{b1} - \phi_{b2} + \phi_{d1} - \phi_{d2}\right] = E_i \cos\left[\pi \frac{(V_{b1} - V_{b2})}{2V_\pi} + \pi \frac{(V_{d1} - V_{d2})}{2V_\pi}\right] \tag{23}$$

As the bias voltage is ½ Vπ, $\phi_{b1} = \pi V_{b1}/V_\pi = \pi/2$. Therefore In phase MZIM is biased at the quadrature point $V_{\pi/2}$. The driving voltage would hence be the cause of fluctuation within 0 to π on the intensity curve. To make the in phase and quadratue MZIM orthogonal, optical carrier frequency is shifted by –3π/2 or 3π/2. The quadrature MZIM operates in a similar manner. However it is biased at zero intensity point. Thus, drive voltage toggles between π/2 to3π/2. The superposition of the outputs of two MZIMs produces the optical MSK signal [20].

The modulated optical signal from the MZIM can vary according to the biasing on the modulator. When the modulator is biased at the maximum or minimum point on the intensity curve, the frequency of the modulated signal is twice the frequency of the driving signal. The duty cycle of the modulated signal is 33% for maximum biasing point. The modulated signal biased at maximum transmission point has the same optical phases at all pulses.

5.2 Signal propagation model

The simulation of the signal propagation is based on the solution of the nonlinear Schrödinger equation and the numerical method used to solve the nonlinear Schrödinger equation is known as the Split-Step Fourier Method (SSFM). The SSFM is based on the division of the fibre into small steps *dz*. Initially, a field (Gaussian pulse in this project) is inserted at the step input. The field at the step output can be determined by applying two operators to the field at the step input: first a linear operator taking into account dispersion (GVD) and attenuation, then a nonlinear operator accounting for the Kerr effect. When the pulse is within a first linear operating region, the model propagates the pulse in frequency domain. Hence the signal is Fourier transformed by means of the FFT multiplied by the transfer function ($e^{-j\beta(\omega)dz_s/2}$) of the fibre piece .Then the resulting signal (U1/2-) is anti-Fourier transformed and multiplied by the operator representing the nonlinearity since pulse in between two linear region (nonlinear region)travels in time domain. At this point, the signal or the pulse is represented as U1/2+. Once this signal enters the second half of the linear region, it is Fourier transformed and multiplied again by transfer function. The resulting signal at this point now represents as U1.Therefore as a pulse propagates through a segmented path; the pulse is switching between frequency and time domain alternatively. When the signal (U1) enters the next segmented path, it becomes the input field (U0) and same process repeats within each segmented path along the fibre span. The process is illustrated in Figure 10 which is integrated in the Simulink model as shown in Figure 9.

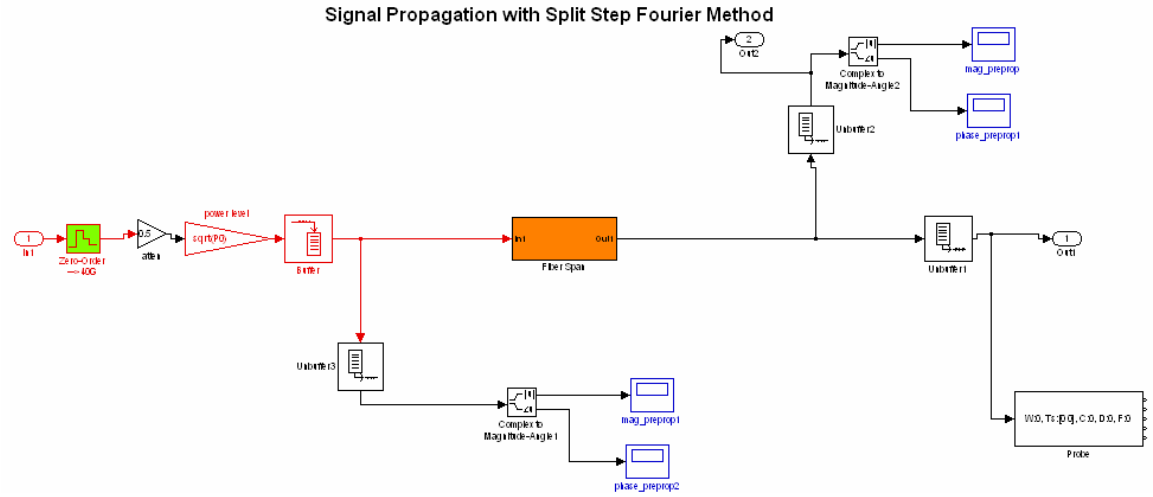

Figure 8: Signal optical fiber propagation model.

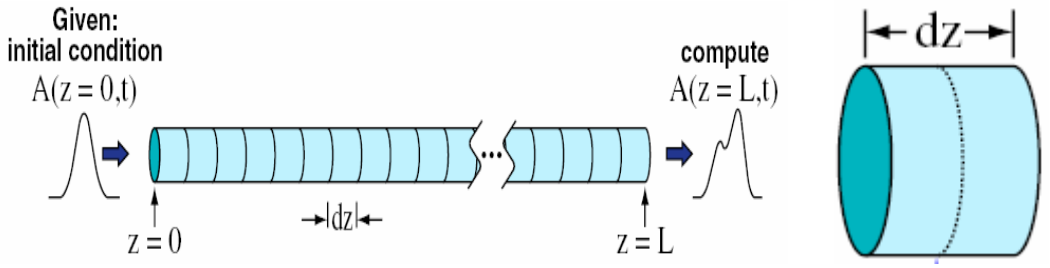

(a) (b)

Figure 9 Fibre structure in SSFM (a) Divide region into small segment of length *dz* (b) approximate nonlinearity as a lumped effect at the centre of each segment. [19]

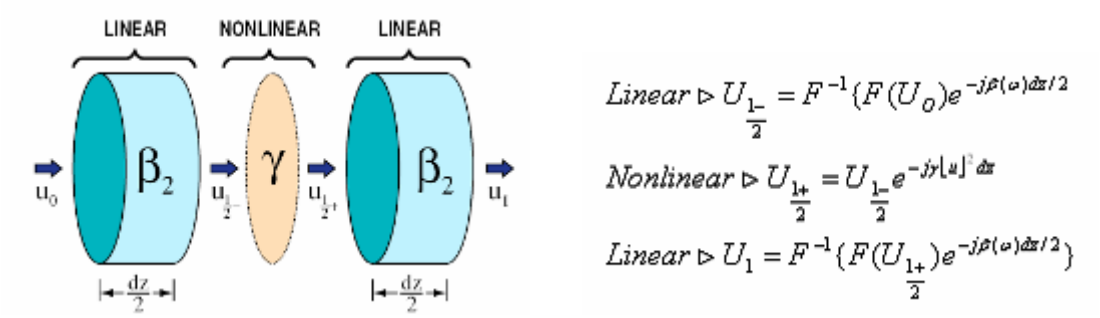

Figure 10: Split step Fourier method [19]

5.3 Single fiber mode

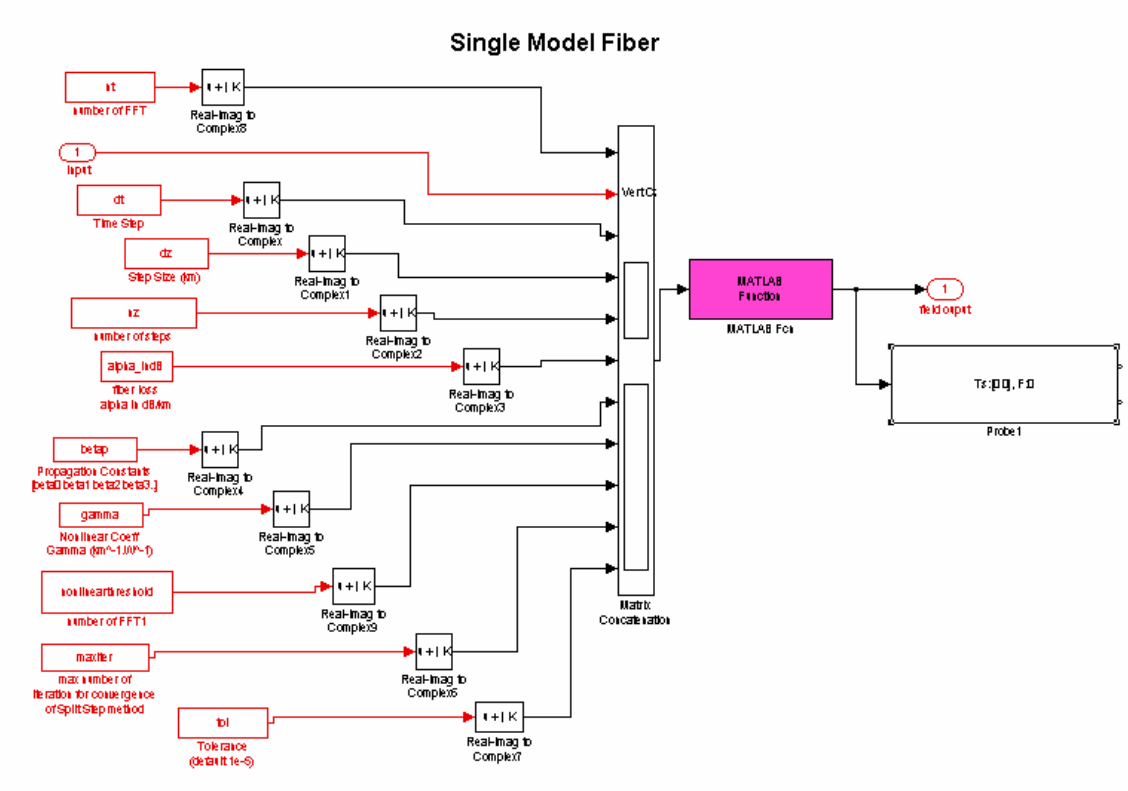

Figure 11: Properties of SMF fibre

The properties of single mode fibre and dispersion compensated fibre such as attenuation, nonlinearity, step size, number of steps are illustrated as parameter blocks using Matlab function. DCF is achieved by changing the dispersion propagation constant to negative and to obtain a mismatched compensation, a ratio is multiplied by step

size parameter. For example, to obtain a mismatch of 1km, the DCF's step size (dz) parameter needs to be (dz*0.9889). The Appendix gives the Matlab code to run for Raman amplification in standard SMF.

Dispersion-compensating fibre DCF is the predominant technology for dispersion compensation. It consists of an optical fibre that has a special design such as providing a large negative dispersion coefficient while the dispersion of the transmission fiber is positive. A proper length of DCF allows the compensation of the chromatic dispersion accumulated over a given length of the transport fibre, although standard modules with predetermined dispersion values are commercially available. The main advantage of the DCF technique is the fact that it provides a broadband operation with a smooth dispersion property and good optical characteristics. In the first generation of DCF, only about 60% of the standard single-mode fibre (SSMF) dispersion slope could be compensated. Now, 100% slope matching for SSMF is commercially available. DCF also presents a quite large insertion loss [8].

5.4 Balance receiver

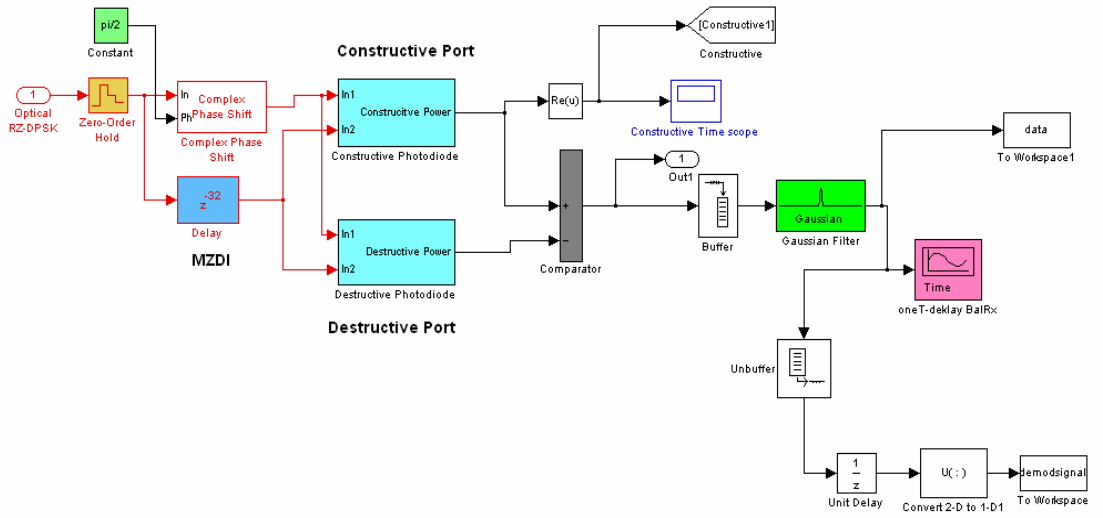

Figure 12: Optical MSK receiver

The role of an optical receiver is to convert the optical signal back into electrical form and recover the data transmitted through the light wave system. Its main component is a photo-detector that converts light into electricity through the photoelectric effect. In general, an optical receiver consists of a high speed photo-detector followed by electronic amplifier and then main amplifier, clock recovery and sampling circuits for the case of amplitude shift keying modulation. However for phase modulation techniques a balanced receiver is needed. A balance receiver consists of a photonic Mach Zehnder delay interferometer (DI) acting as a phase comparator and detected by two photo detectors connected back to back then a single input electronic pre-amplifier or fed to a differential electronic amplifier.

The main mechanism of MSK receiver is to detect the phase difference between two bits; whether it's in phase or Q- signal—that is what detectors needs to find out. A simple non-coherent configuration for detection of a linear and nonlinear optical MSK sequences consists of the well known integrated optic phase comparator Mach-Zehnder Delay Interferometer (MZDI) balanced receiver with one-bit time delay on one arm of MZDI [20]. An additional $\pi/2$ phase shift is introduced to detect the differential pi/2 phase shift difference of two adjacent optical MSK pulses. The outputs of the phase shifted signal and delayed signal link to two photo detectors. One photo detector is constructive and another is destructive. The two input signal of a photo detector interfere with each other. If the interference is constructive, a presence of power is experienced at the photo detector. Likewise, an absence of power indicates the destructive interference .Therefore ,it can be stated that the destructive interference cause by the phase difference of π, which is a logic "0" signal and constructive interference indicate logic "1'.

5.5 Numerical modeling and performance

A Matlab numerical modelling has been generated yielding optical pump power, signal power and Raman contributed gain which are then fetched into the propagation section of the Simulink model .The propagation program has been created in order to add Raman gain into the Split-Step Fourier Method .

To model Raman configurations such as forward, backward and bi-directional, an analytical solution was derived from the coupled equations ignoring the pump depletion. Two ode45 functions were produced for backward and forward pumping respectively. This was achieved by changing the pump direction. To investigate whether NLS equation has successfully incorporated the Raman gain and using the SSFM propagation program, a single Gaussian pulse has been integrated into the system as input field. The peak power of the Gaussian pulse has set to be 1mW. Every pump configurations has been modelled with a span of 90km, using step size of 450m and 200 steps.

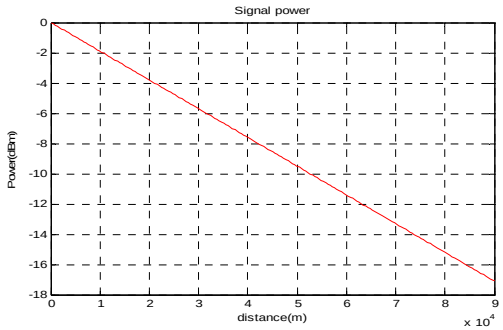

Figure 13Attenuation map of a passive fibre over the total length of 90km without amplification, α = 0.19dB/km.

5.5.1 Forward pumping

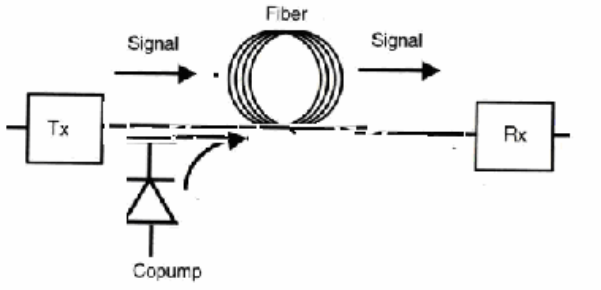

Figure 14: Forward pumping Configuration

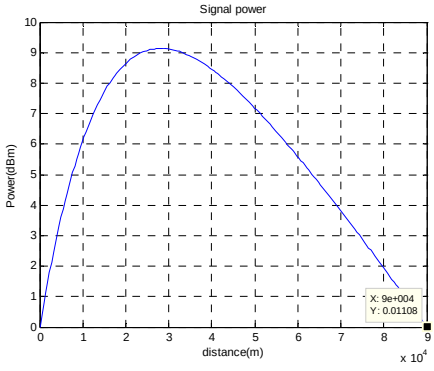

Figure 15 Signal power progress along the fibre under forward pumed Raman amplification.

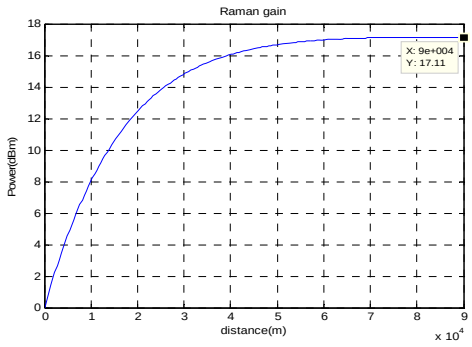

Figure 16 Raman gain contribution along the fibre under forward pumping

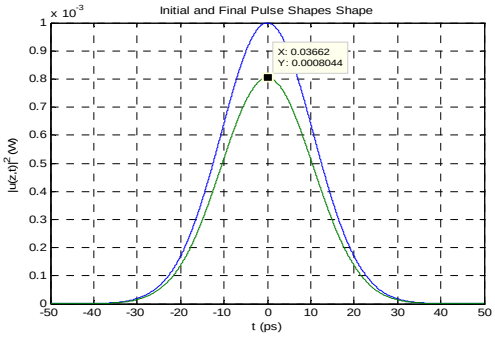

Figure 17 Gaussian input and output pulse for the case of forward pumped optical amplification.

In all the Gaussian testing cases presented throughout the results section, the input pulse is represented in blue and the output in green .The output of the signal obtained from the end of the fibre is 0.01dB as refer to forward pumping signal graph whereas a final pulse of 0.8044mW is obtained from Gaussian graph which correlate 10log (0.8044/1) = -0.945 dB as shown in Figure 17. Hence there is a slight variation between the two functions.

5.5.2 Backward pumping

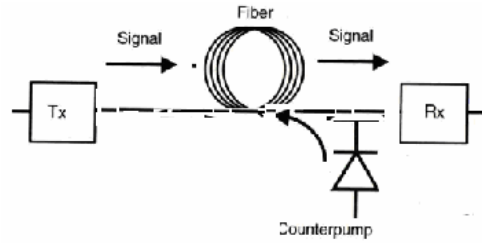

Figure 18 Backward pumping configuration

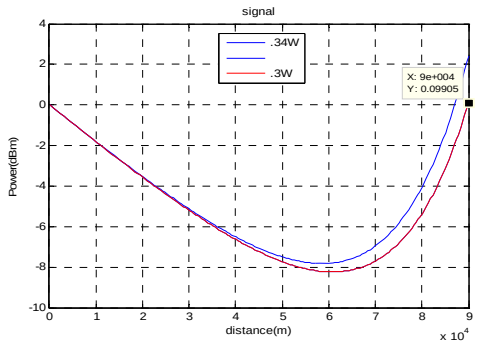

Figure 19: Signal power progress along the fibre: Backward pumping Red and blue representing pump power of 300mW and 340mW respectively.

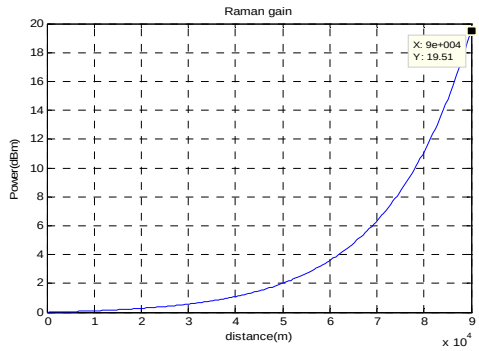

Figure 20: Raman gain contribution along the fibre for backward pumping.

5.5.3 Bi-direction Configuration

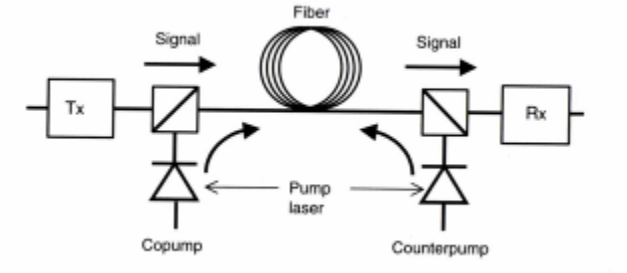

Figure 21: Bi-directional pumping configuration

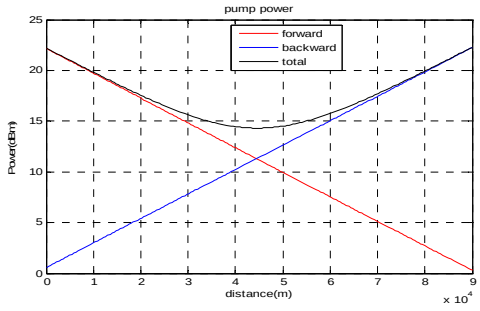

Figure 22: Pump power evolution: 165mW of forward and backward pumping represents in red and magenta respectively. Black represents bi-directional pump power when pump is provided from both ends.

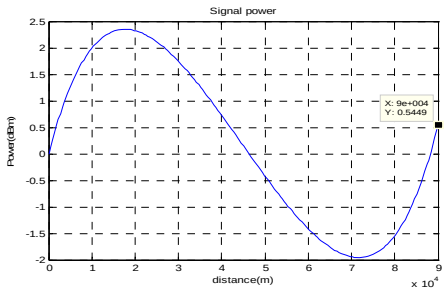

Figure 23: Signal power progress along the fibre: Bi-Directional Pumping

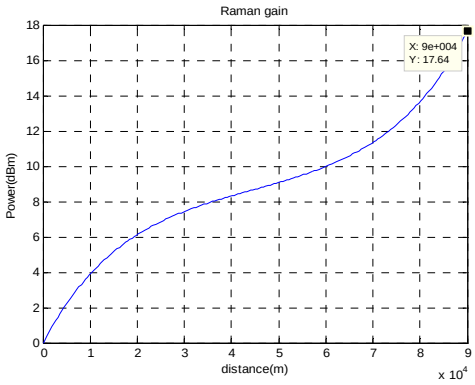

Figure 24: Raman gain contribution along the fibre for bi-directional pumping

The gain contribution by Raman amplifier equalise the total power loss at the end of the fibre experiencing the absences of Raman amplifier. This is also known as on-off gain. For instance, a 90km fibre has total power loss of (90*0.19=17.1dB) it requires a Raman gain of more than 17.1dB to compensate such attenuation (fibre loss). Given that Raman is a distributed amplifier, the gain at each point along the fibre is different. Thus the gain curve as shown in Figure 24.

As mentioned above that Raman gain is integrated into the Split-Step Fourier procedure to simulate the transmission of signal over fibr. Considering SSFM takes place in every step along the fibre, it is necessary to compute Raman gain contribution at each step. By comparing gain contribution at two points, the gain has been converted as a gradient. As the attenuation due to the signal is constant over the fibre, it can be considered that each step would have constant gradient of attenuation. Subsequently the propagation program has included two square matrixes: one contains Raman gain and other one contains attenuation. Then they are added and stored in one matrix. This matrix has a nominal size of 200 values containing 200 Raman contributed steps along the fibre. When first step of the fibre is under SSF process, the program is commanded to access the first value of the matrix. While SSFM process goes to second step of the fibre, program accesses second value of the matrix. Such process continues up to 200th step for a Raman amplified section as shown in the Raman programs in the Appendix.

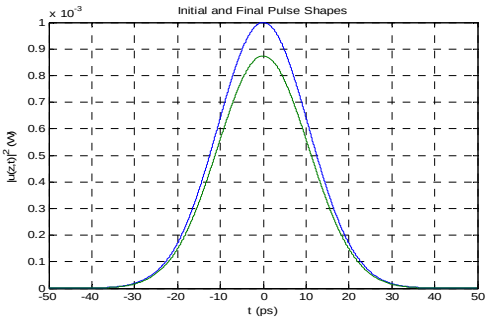

Figure 25: Gaussian input and output pulse for the case of bidirectional pumping

In Figure 25, input pulse is 1 mW and the output is 0.8737 mW. At the end of the fibre the expected output is 0.5449 dB as it is clearly seen from the signal power graph. To verify whether the output achieved from the split-step method is accurate, output Gaussian pulse needs to be converted into decibel form. The peak at the output is 0.8737 mW, which is 10log (0.8737 /1) = -0.5863 dB. Thus there is a slight mismatch between the two functions.

5.5.4 Reverse bi-directional (mid-span) pumping

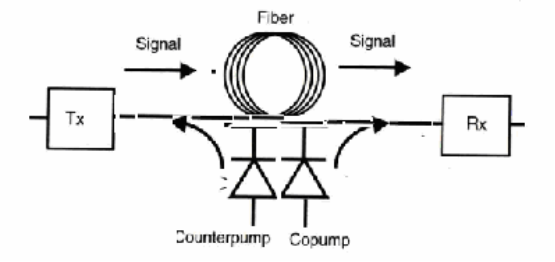

Figure 26: Mid-span pumping configuration

Reverse bi-directional pumping quite similar to bi-directional pumping in term of pump power arrangement; launching 165mW power from the middle of the span at opposite direction. In addition, exactly same numerical gain contribution that has been used for bi-directional configuration, also applied in this case to incorporate with propagation program. However the gain contribution order is changed.

To fashion such configuration, the span is considered into two halves. 1st half is experiencing a backward pump over the fibre length of 45 km and 2nd half experiencing a forward pump over the fibre length of 45 km. For each half of the span, 165mW pump has been provided to obtain a net gain of 0 or more at the end of 45km.Step number of 100 is implemented in numerical gain MATLAB function in this case; so as Gaussian pulse to test model's accuracy.

Such testing confirms the fact that reverse bi-directional configuration can be derived from the bi-directional by changing the order of gain contribution along the fibre. In other words, by shifting the gain contribution from the 2nd half of the span to the 1st half of the span and vice versa. In order to do so, the last 100 values of the Raman contributed matrix were shifted to the front and stored.

After the matrix shifting, a Gaussian pulse can be added to test the pulse generation along the span. The table below tabulates the Gaussian peak power at every ten steps to compute the signal power along the fibre.

At each No of step	Bidirectional power(mW)	power(dBm)	Mid-span power(mW)	power(dBm)
1	0.9795	-0.089955597	0.9795	-0.089955597
10	1.269	1.034616221	0.8456	-0.728350257

20	1.481	1.705550585	0.776	-1.101382787
30	1.595	2.027606874	0.6963	-1.572036048
40	1.615	2.081725267	0.6353	-1.970211447
50	1.559	1.928461152	0.5954	-2.251911697
60	1.452	1.619666164	0.5786	-2.376215707
70	1.32	1.205739312	0.5899	-2.292216038
80	1.179	0.715138051	0.6404	-1.935486768
90	1.041	0.174507295	0.7543	-1.224558923
100	0.9145	-0.388162902	0.987	-0.056828473
110	0.804	-0.947439513	1.227	0.888445627
120	0.7112	-1.48008252	1.445	1.598678471
130	0.6368	-1.959969453	1.567	1.950689965
140	0.581	-2.358238676	1.595	2.027606874
150	0.5443	-2.641616657	1.546	1.892094896
160	0.5291	-2.764622385	1.446	1.60168293
170	0.5395	-2.68008551	1.317	1.19585775
180	0.5856	-2.323989319	1.177	0.707764628
190	0.6898	-1.6127681	1.04	0.170333393
200	0.8737	-0.586376643	0.9144	-0.388637826

Table 1: Signal power at every ten steps in reverse bi-directional pumping

Mid-span pumping is more efficient since Gaussian peak power at the end of the fibre length is higher. The Raman gain is higher at the middle of the fibre span (at 45km) where the Raman pump sources are coupled. In standard bi-directional scheme, the gain contribution is higher at the beginning and end of the span and hence nonlinearity may occur and limit the signal launched power.

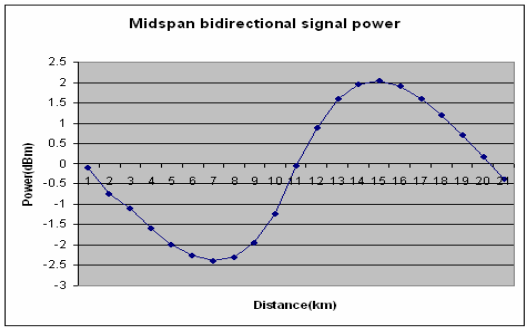

Figure 27: Signal power progress along the fibre: Mid-span pumping

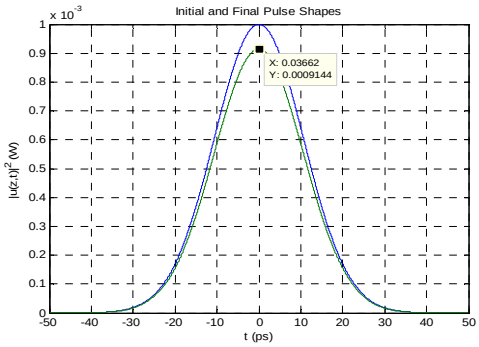

Figure 28: Gaussian input and output pulse for the case of mid-span pumping

The output of the signal obtained from the end of the fibre is 0.5449 dB which is same as bi-directional signal graph since same numerical parameters been used. However the output as seen by the graph above is 0.9144 mW. This in turn correlates to a gain of 10log (0.9144/1) = -0.3886 dB. So there is a slight difference between the two functions.

A small mismatch between Numerical and Gaussian representation are existed in all the pumping techniques described above. Aspects influencing such mismatch are mainly the numerical approximation of the gain curves, the gradients used from the gain curves and the implementation of the FFT used to solve the NLSE.

5.5.5 Transmission performance

The performance of the model has been analysed integrating BER under different condition such as input power of the signal, number of span and mismatching compensated fibre. The area where the eye opening is maximum, normally only 40% to 60% region of the middle of eye, has been sampled to estimate the BER, using SIMULINK workspace histogram and the Matlab file included in the Appendix.

In the simulation model, a span length of 180km has been used to propagate signal for linear MSK (90km of SMF and 90km of DCF).EDFA and Raman amplifier are incorporated in MSK model to evaluate the best performance configuration. For EDFA scheme, a gain of 16 dB and 4dB noise figure is applied at the end of 90km SMF and 90km DCF. Five different Raman pumping has also been tested with linear MSK model such as forward, backward, conventional bi-directional, Mid-span bi-directional and hybrid pump configuration. Pump power of 165mW has been launched from each pump according to pump configuration. In the cases of forward and backward pumping 340mW pump power has been instigated.

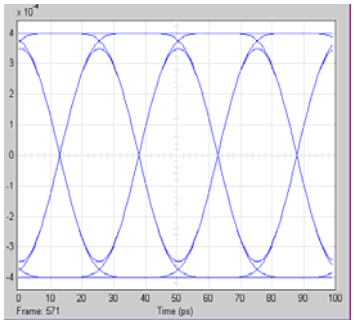

Figure 29: Back to back eye diagram.

Initially the model has been tested under back-to-back system. Figure 29Figure 36 shows the non-distorted 40Gb/s signal that is expected at the end of receiver. Clearly the signal is noise free given that no fibre constraints

are influenced. The pulse width is 25 ps, which is the expected result after the initialization file is run. This corresponds to a 40 Gb/sec transmission rate.

5.5.6 Optically amplified non-compensated fiber spans

The dispersion effects in fibre are then investigated by inserting the number of optically amplified spans of length of 180km. Distortion at sampling time and distortion at zero crossing increase with the number of spans. Not only so, non linear affects also take place since the shape of the eye starts to become asymmetric. After one span of propagation with EDFA, Bidirectional Raman and Mid-span Raman correspond to a BER of 1e-38, 1e-39,1e-45 respectively. A BER lower than 10^{-9} is obtained for hybrid EDFA and Mid-span pump with propagated distance up to 540km; however Bi-directional allows propagating up to 720km in such condition.

Span	EDFA	B-directional	Mid-span		Backward	Forward
1	1.00E-38	6.50E-39	1.30E-45		3.83E-53	3.90E-18
2	1.00E-22	4.40E-34	2.40E-27		1.00E-35	2.90E-07
3	1.00E-13	2.40E-27	7.30E-15		2.30E-19	X
4	1.00E-08	1.58E-10	2.83E-08		1.70E-17	X
5	X	1.50E-06	2.50E-06		1.49E-12	X
6	X	1.80E-03	1.10E-03		3.80E-09	X
7	X	X	X		1.30E-06	X
8	X	X	X		1.00E-03	X

Table 2: BER measured at the end of each span.

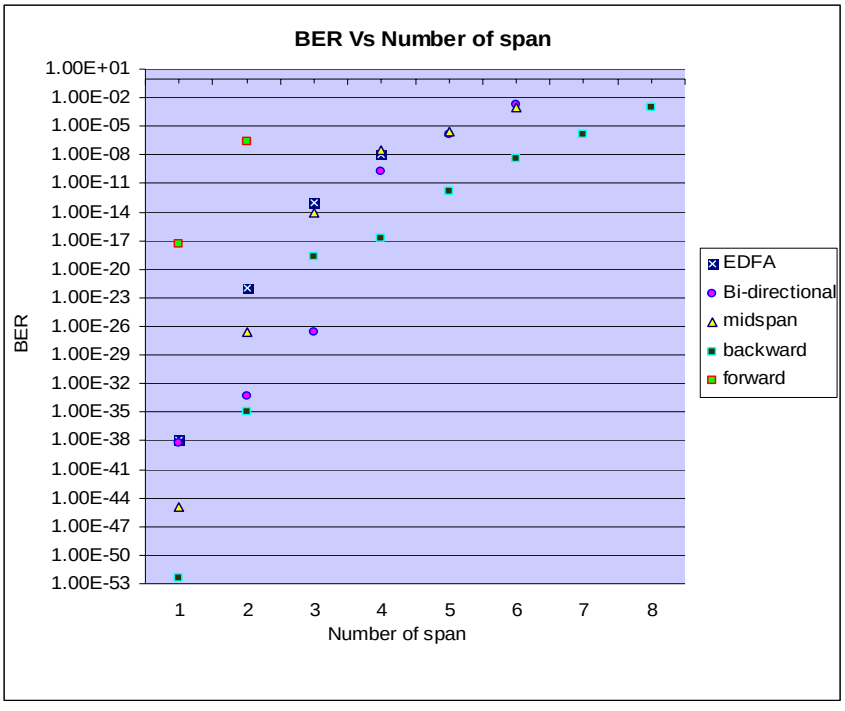

Figure 30: BER versus Number of span (180 km DC span)

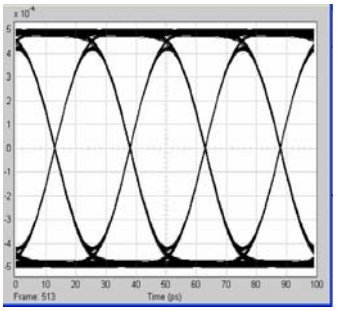

Figure 31 Eye diagram for linear MSK with conventional Bi-directional Raman pumping configuration after one SSMF span of propagation.

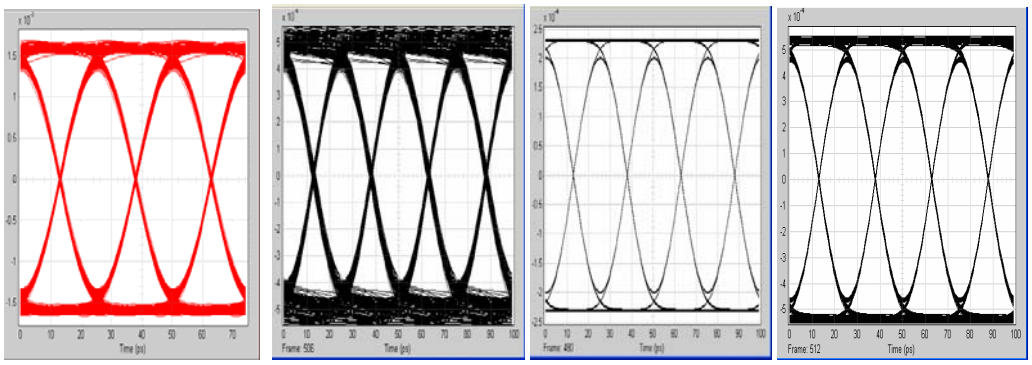

(a) (b) (c) (d)

Figure 32: Eye diagram for linear MSK with (a) EDFA (b) forward Raman pumping (c)Backward Raman pumping (d) Mid-span Raman pumping, after one span of propagation.

5.5.7 Optically amplified compensated Fiber spans

In order to investigate the tolerance of the models to dispersion, the simulations with compensation mismatch of 1km and 2km have been carried out. All the models are not tolerant to compensation mismatch as the BER for are higher than 10^{-9}.

In EDFA and Raman configuration, BER starts to decrease as the distance of mismatched dispersion compensation increases. In this case, results satisfy the theory where fully compensated system should produce a better BER since dispersion in the fibre is fully reduced. The result shows that Raman pumping is more sensitive than EDFA in both Bi-directional and Mid-span configuration.

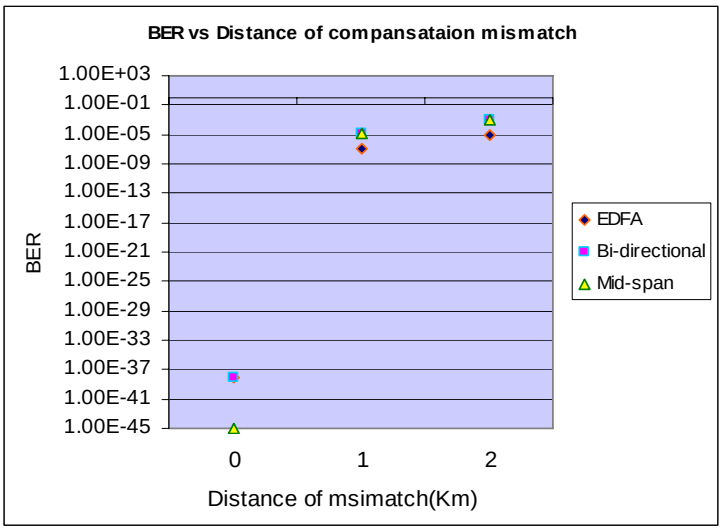

Figure 33: BER versus SSMF distance of compensation mismatch

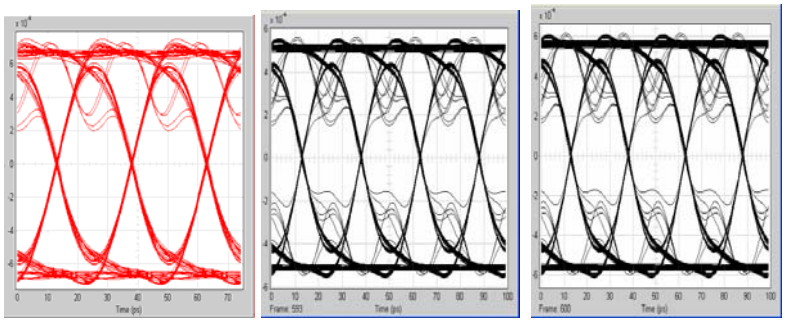

(a) (b) (c)

Figure 34 Eye diagram for Linear MSK using (a) EDFA (b) bi-directional Raman pump and (c) mid-span Raman pump, with 1km of dispersion compensation mismatch

5.5.7.1 Input signal power

The tolerance of the models to nonlinear effects is tested by increasing the input power into the fibre span, keeping the length 180km. More power would cause more noise in fibre and at the conversion of photocurrent .The nonlinear phase shift is proportional to the input power, thus increasing the input power increases nonlinear phase shift additionally. This nonlinear phase shift is observed through the asymmetries in the eye diagram.

Initially Raman amplification has been tested with an input power of 1mw. However the signal did not propagate after 180km span. The reason is Raman amplifier amplifies signal through out fibre. At the beginning of the fibre where the signal is strong; forward or bi-directional configuration would take such higher signal to nonlinear regions.

Subsequently 0.1mW signal power is launched which propagated up to 1080km (six spans) with the help of mid-span and bi-directional configuration. On the other hand EDFA can tolerate with an initial signal power up to 6mw, providing a BER of 1e-12.This is due to the its lumped behaviour, since EDFA amplifies an attenuated(weaker)signal. Further investigation has been conducted to test the tolerance level of Raman amplifiers. Result shows signal power of 0.5mw can be achieved for a propagation distance of 180km with BER of 1e-12. With a signal power of 0.3mW and 0.2mW, propagation distance of 720km and 540 km are accomplished respectively.

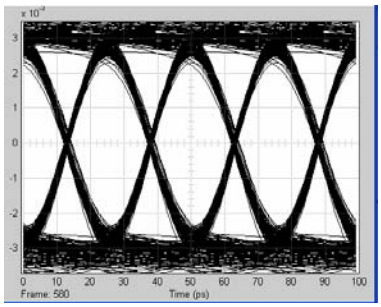

Figure 35: Linear MSK with Bi-directional pumping after a single span with -3dBm signal launched power.

5.5.7.2 Hybrid optical amplified transmission

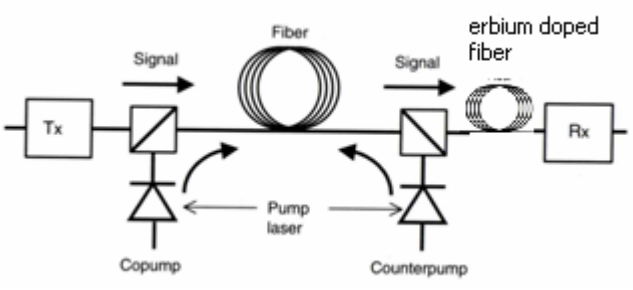

Figure 36: Hybrid pumping configuration

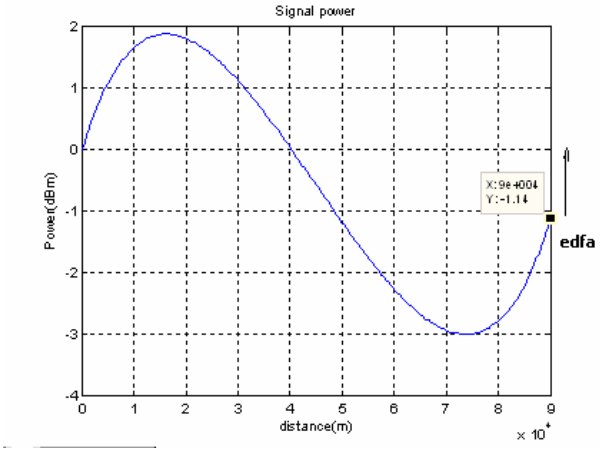

Figure 37 Signal power evolution in hybrid configuration

Hybrid transmission systems involve both Raman and EDF amplifiers. Mid-span and booster EDFAs are inserted after both the SM and DC fibres. The length of the fibre is 90 km (span length=180km) and the pump power was decreased to 150mW in the forward -backward direction. Thus the gain required by the EDFAs is 1.14dB to obtain a net gain of 0.A propagation distance of 360km and 540km are used to compare the quality of signal with standalone EDFA and Raman pumped system.

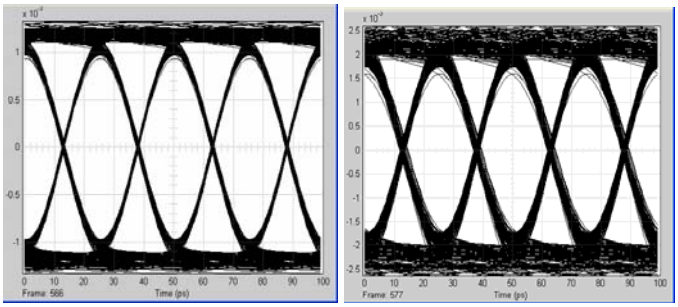

(a) (b)

Figure 38: Hybrid optical amplification (a) after 360km propagation (b) after 540km propagation

Number of Spans	EDFA	B-directional	Mid-span	hybrid
2	1.00E-22	4.40E-34	2.40E-27	4.85E-19
3	1.00E-13	2.40E-27	7.30E-15	5.30E-11

Table 3: BER comparison between hybrid and single direction Raman pumping configuration over 360km and 540km span.

The result shows that hybrid system provides less quality signal in contrast to fully EDFA or Raman system .However the quality difference between EDFA and hybrid are approximately a BER factor of 100. In such comparison, Raman makes a significant improvement in system quality.

6 Conclusion

Raman amplification has been implemented with MSK modulation format for 40Gbit/s long-haul transmission. Comparison between Raman and EDFA system are accomplished using Matlab Simulink simulation model. Under several conditions, Raman amplification proves to be an efficient signal enhancement for linear MSK modulation format.

A BER of better than 10^{-11} is achieved over a propagation distance of 540km with EDFA amplification and fully dispersion compensated fibre multi-span. A BER of better than 10^{-10} is achieved over propagation distance of 720km with bi-directional Raman amplification and fully dispersion compensated fibre multi-span. A propagation length of 1080km can be integrated into system with -10dBm signal power using Mid-span and Bi-directional Raman pump configuration. Propagation length of 1440km and 360km can be integrated into system with -10dBm signal power using Backward Raman and Forward Raman configuration respectively. It has been shown, by simulation, that Raman amplification can enhance the MSK modulated optical transmission systems under the CD dispersion and nonlinear effects. Consequently MSK is potentially a much preferred modulation format for long–haul DWDM optical communication incorporating Raman amplification.

7 Reference

[1] [1] G.P. Agrawal, “Nonlinear Fiber Optics,” 2nd ed., Academic Press, San Diego, CA, 1995.

[2] [2] G.P. Agrawal, “Fiber-Optic Communication Systems,” 2nd ed., Wiley, New York, NY, 1997.

[3] L.N. Binh and TL Huynh, “Hybrid 40G Overlay 10G DWDM Photonic Transmission Systems Using Advanced Modulation Formats”, OFC 2007.

[4] M. Ohm and J. Speidel, “Optical Minimum-Shift Keying with Direct Detection (MSK/DD),” in Proc. of SPIE 2004, vol. 5281, pp. 150-161.

[5] A.H. Gnauck and P.J. Winzer, “Optical Phase-Shift Keyed Transmission,” IEEE J. Lightw Tech., vol. 23, pp. 115-130, 2005.

[6] L.N. Binh, T.L. Huynh and H.S. Tiong, ”DPSK RZ Modulation Formats Generated From Dual Drive Electro-photonic Modulators”, Technical report, ECSE Monash university, 2005.

[7] Mohammed N. Islam “Raman Amplifiers for Telecommunications”

[8] Jinyo Mo and Yi Dong “Optical minimum shift keying for high spectral efficiency WDM system”

[9] K K Pang, “ECE 4406 Digital transmission”, Monash University, MiTech Pub, 2002.

[10] M. K. Simon, P. Arabshahi,1 L. Lam, and T.-Y. Yan, "Power Spectrum of MSK-Type Modulations in the Presence of Data Imbalance" TMO Progress Report 42-134, University of Washington, August 15, 1998.

[11] Subbarayan Pasupathy, "Minimum Shift Keying: A Spectral Efficient Modulation", IEEE Communications Mgazine,Vol.17,No.4, pp. 14- 22, 1979.

[12] by Takahide Sakamoto, Tetsuya Kawanishi, and Masayuki Izutsu, "Optical minimum-shift keying with external modulation scheme"

[13] Le Nguyen Binh, "Optical receivers lecture notes ece4405/ece5405 optical communications systems", MItec Pub, Melbourne 2002.

[14] K.P. Ho, "Phase modulated optical communication system", Academic Press, 2005.

[15] R. S. Kaler "Comparison of various dispersion-compensation techniques in a cable television system",

[16] RED-C Optical Networks Ltd PDF: White paper

[17] SHF Communications Technologies AG :http://www.shf.biz

[18] T. E. Murphy, "Soliton Pulse Propagation in Optical fibre" ,MIT Lincoln Laboratory .

[19] T.L. Huynh, L.N. Binh, K. K. Pang, and L. Chan, "Photonic MSK transmitter models using linear and nonlinearphase shaping for non-coherent long-haul optical transmission." , Technical report, ECSE Monash University, 2005.

[20] K.P. Ho, "Advanced Topics in Lightwave Communications Generation of Optical Signals," 2005.

[21] Headley, C & Agrawal, G P. "Raman Amplification in Fibre Optical Communication Systems", Elsevier Inc., 2005.

8 Appendix

8.1 Initialization m-file:SMF_Q_Initialisation_ssprop_SIunit.m

```
% This file solves NLSE for
% pulse propagation in an optical fiber using the split-step
% Fourier method as given in: GP. Agrawal,"Nonlinear Fiber Optics", 2nd ed.
% AP, 1995, Chapter 2
%
% The following effects are included in the model: group
% velocity dispersion (GVD), GVD-slope / third-order
% dispersion, loss, and self-phase modulation (n2).  The core
% routine is implementing the split-step propagation
close all
clear all
 % CONSTANTS
c = 3e8;                          % speed of light (m/s)
% NUMERICAL PARAMETERS
numbitspersymbol = 1;
P0 = 0.0001;                               % peak power (W)
FWHM =  25e-12  ;                             % pulse width FWHM (ps)
FWHMps = 25e-12;
%halfwidth = FWHM/1.6651                % for Gaussian pulse
halfwidth = FWHM     ;                  % for square pulse
bitrate = 1/halfwidth;                  % THz
bitrateG = 1/FWHMps;
baudrate = bitrate/numbitspersymbol;
signalbandwidth = baudrate;
%%%%%%%%%%%%%%%%%%%%%%%%%%%%%%%%
%%%%%%%%%%%%%%%%%%%%%%%%%%%%%%%%
PRBSlength = 2^6;
% Make sure : FFT time window (=nt*dt) = PRBSlength * FWHM...
% FFTlength nt = PRBSlength/block * numbersamples/bit = PRBSlength * (FWHM/dt)
% num_samplesperbit = FWHM/dt  should be about 8 - 16 samples/bit
num_samplesperbit = 32;                % should be 2^n
```

```
    dt = FWHMps/num_samplesperbit ;           % sampling time(ps); % time step (ps)
    nt = PRBSlength*num_samplesperbit;      % FFT length
    dz = 450;                               % distance stepsize (m)
    nz =  200;                                 % number of z-steps
    maxiter = 20;                           % max # of iterations
    tol = 1e-5;                             % error tolerance

    % OPTICAL PARAMETERS
    nonlinearthreshold = 0.000000005; % 5mW -- % Nonlinear Threshold Peak Power for silica core
fibre
    ambda = 1550e-9;
    % lambda_carrier = 14648.4375;           % wavelength (nm)with
    %Level 4 group the carrier freq is scaled down to 500G or 200 GHz
    optical_carrier = c/lambda;      %carrier freq
    %num_samplesperperiod = 8;
    %sampling_fac =  16;
    num_samplesperperiod = 8;
    sampling_fac =  16;
    carrier_freq = num_samplesperperiod*num_samplesperbit*bitrateG;      % artificial freq
    %dt = FWHM/(num_samplesperbit*num_samplesperperiod*sampling_fac) ;           % sampling
time(ps); % time step (ps)
    %nt = PRBSlength*num_samplesperbit*num_samplesperperiod*sampling_fac ;      % FFT length
    %dBperkm = 0.2;                          % loss (dB/km)
    alpha_indB = 0.2;                          % loss (dB/km)
    D = 17e-6;                                 % NZDSF GVD (s/m^2); if anomalous dispersion(for
compensation),D is negative
    %D = 17;                                 % SSMF GVD (ps/nm.km); if anomalous dispersion(for
compensation),D is negative
    ng = 1.46;                              % group index
    n2 = 2.6e-20;                           % nonlinear index (m^2/W)
    Aeff = 80e-12;                          % effective area (um^2)
    % CALCULATED QUANTITIES
    T = nt*dt;                              % FFT window size in sec. (ps) -Agrawal: should be
about 10-20 times of the pulse width
    alpha_loss = log(10)*alpha_indB/10^4;     % alpha (1/m)
    beta2 = D*lambda^2/(2*pi*c);            % beta2 (s^2/m);
    beta3 = 0.3e-39;                        % GVD slope (s^3/m)
    %beta2 =0;
    %-----------------------------------------------------
    % beta 3 can be calculated from the Slope Dispersion (S) as follows:]
    % Slope Dispersion S = 0.092;           % ps/(nm^2.km)
    % beta31 = (S - (4*pi*c./lambda.^3))./(2*pi*c./lambda.^2)
    %-----------------------------------------------------
    gamma = 2*pi*n2/(lambda*Aeff);       % nonlinearity coef (m^-1.W^-1)

    % STARTING FIELD
    L = nz*dz
    Lnl = 1/(P0*gamma)                    % nonlinear length (m)
    Ld = halfwidth^2/abs(beta2)           % dispersion length (m)
    N = sqrt(abs(Ld./Lnl))                % governing the which one is dominating: dispersion or
Non-linearities
    ratio_LandLd = L/Ld                    % if L << Ld --> NO Dispersion Effect
    ratio_LandLnl = L/Lnl                  % if L << Lnl --> NO Nonlinear Effect
```

```
% Monitor the broadening of the pulse with relative the Dispersion Length
% Calculate the expected pulsewidth of the output pulse
% Eq 3.2.10 in Agrawal "Nonlinear Fiber Optics" 2001 pp67
FWHM_new = FWHM*sqrt(1+(L/Ld)^2);
% N<<1 --> GVD ; N >>1 ---> SPM
Leff = (1-exp(-alpha_loss*L))/alpha_loss;
expected_normPout = exp(-alpha_loss*2*L);
NlnPhaseshiftmax = gamma*P0*Leff ;
betap = [0 0 beta2 beta3]';
%Constants for ASE of EDFA
% PSD of ASE: N(at carrier freq) = 2*h*fc*nsp*(G-1) with nsp = Noise
% Figure/2 (assume saturated gain)
%*************** Standdard Constant ******************************
h = 6.626068e-34;       %Plank's Constant
%***************************************
```

8.2 SSFM: ssprop_matlabfunction_raman_midspan.m

```
function output = ssprop_matlabfunction_raman_midspan(input)

nt = input(1);
u0 = input(2:nt+1);
dt = input(nt+2);
dz = input(nt+3);
nz = input(nt+4);
alpha_indB = input(nt+5);
betap = input(nt+6:nt+9);
gamma = input(nt+10);
P_non_thres = input(nt+11);
maxiter = input(nt+12);
tol = input(nt+13);
%Ld = input(nt+14);
%Aeff = input(nt+15);
%Leff = input(nt+16);

tic;
%tmp = cputime;
%-------------------------------------------------------------
% Original author: Thomas E. Murphy (tem@alum.mit.edu)
% Adapted and modified by Thanh Liem Huynh (thanh.huynh@eng.monash.edu.au)
%-------------------------------------------------------------
% This function ssolves the nonlinear Schrodinger equation for
% pulse propagation in an optical fiber using the split-step
% Fourier method described in:
%
% Agrawal, Govind.  Nonlinear Fiber Optics, 2nd ed.  Academic
% Press, 1995, Chapter 2
%
% The following effects are included in the model: group velocity
% dispersion (GVD), higher order dispersion, loss, and self-phase
% modulation (gamma).
%
```

```
    % USAGE
    %
    % u1 = ssprop(u0,dt,dz,nz,alpha,betap,gamma);
    % u1 = ssprop(u0,dt,dz,nz,alpha,betap,gamma,maxiter);
    % u1 = ssprop(u0,dt,dz,nz,alpha,betap,gamma,maxiter,tol);
    %
    % INPUT
    %
    % u0 - starting field amplitude (vector)
    % dt - time step - [in ps]
    % dz - propagation stepsize - [in km]
    % nz - number of steps to take, ie, ztotal = dz*nz
    % alpha - power loss coefficient [in dB/km], need to convert to linear to have P=P0*exp(-
alpha*z)
    % betap - dispersion polynomial coefs, [beta_0 ... beta_m] [in ps^(m-1)/km]
    % gamma - nonlinearity coefficient [in (km^-1.W^-1)]
    % maxiter - max number of iterations (default = 4)
    % tol - convergence tolerance (default = 1e-5)
    %
    % OUTPUT
    %
    % u1 - field at the output
    %---------------
    % Convert alpha_indB to alpha in linear domain
    %---------------
    alpha = 1e-3*log(10)*alpha_indB/10;          % alpha (1/km) - see Agrawal p57
    %---------------
    %P_non_thres = 0.0000005;

    ntt = length(u0);
    w = 2*pi*[(0:ntt/2-1),(-ntt/2:-1)]'/(dt*nt);
    %t = ((1:nt)'-(nt+1)/2)*dt;

    gain = numerical_gain_midspan(dz,nz);

    for array_counter = 2:nz+1
        grad_gain(1) = gain(1)/dz;
        grad_gain(array_counter) = (gain(array_counter)-gain(array_counter-1))/dz;
    end
    gain_lin = log(10)*grad_gain/(10*2);

    clear halfstep
      halfstep = -alpha/2;
        for ii = 0:length(betap)-1;
            halfstep = halfstep - j*betap(ii+1)*(w.^ii)/factorial(ii);
        end
         square_mat = repmat(halfstep, 1, nz+1);
         square_mat2 = repmat(gain_lin, ntt, 1);
         size(square_mat);
         size(square_mat2);
         total = square_mat + square_mat2;
```

```
     tot= circshift(total,[0,100]);%shifting matrix last 100 to left
clear LinearOperator
    % Linear Operator in Split Step method
    LinearOperator = halfstep;
    halfstep = exp(tot*dz/2);
u1 = u0;
ufft = fft(u0);

% Nonlinear operator will be added if the peak power is greater than the
% Nonlinear threshold
iz = 0;
while (iz < nz) && (max((gamma*abs(u1).^2 + gamma*abs(u0).^2)) > P_non_thres)
  iz = iz+1;
  uhalf = ifft(halfstep(:,iz).*ufft);
for ii = 1:maxiter,
    uv = uhalf .* exp((-j*(gamma)*abs(u1).^2 + (gamma)*abs(u0).^2)*dz/2);
    ufft = halfstep(:,iz).*fft(uv);
    uv = ifft(ufft);

    if (max(uv-u1)/max(u1) < tol)
      u1 = uv;
      break;
    else
      u1 = uv;
    end

  end
  fprintf('You are using SSFM\n');
  if (ii == maxiter)

    warning(fprintf('Failed to converge to %f in %d iterations',tol,maxiter));
  end

  u0 = u1;

end

if (iz < nz) && (max((gamma*abs(u1).^2 + gamma*abs(u0).^2)) < P_non_thres)

%  u1 = u1.*rectwin(ntt);
   ufft = fft(u1);
   ufft = ufft.*exp(LinearOperator*(nz-iz)*dz);
   u1 = ifft(ufft);

   fprintf('Implementing Linear Transfer Function of the Fibre Propagation');
end

%toc;

output = u1;
```

8.3 numerical_gain_midspan.m

```
function gain = numerical_gain_midspan(dz,nz)

%clear all
%close all
%clc

function dpfdz = f(z,p)

dpfdz = zeros(4,1);

%Parameters
ws = 193.3e12;
wp = 206.5e12;
alphas = 0.19/1000; %dB/m
alphap = 0.24/1000; %dB/m

if rf > 0;
    alphas_lin = alphas/4.343;
else
    alphas_lin = 0;
end

alphap_lin = alphap/4.343;

gR_eff = 0.72/1000;
Aeff = 80e-12;
gR = gR_eff*Aeff;%gR_eff*Aeff;
Psf = p(1,:);
Ppf = p(2,:);
Nsf = p(3,:);
Npf = p(4,:);

%Evaluate coupled equations
dpfdz(1) = ((-alphas_lin*Psf+(gR/Aeff)*Ppf*Psf)); % Signal evolution
dpfdz(2) = ((-alphap_lin)*Ppf - (wp/ws)*(gR/Aeff)*Psf*Ppf); % Pump evolution
dpfdz(3) = (-
alphas_lin*Nsf+(gR_eff)*Ppf*Nsf)+(gR_eff)*((2*Ppf*Npf)^(1/2))*Psf+(alphas_lin+(gR_eff)*Ppf)*(h*ws
/2)*Bo;
dpfdz(4) = -alphap_lin*Npf-
((wp/ws)*(gR_eff)*Psf)*(2*Ppf*Npf)^(1/2)+alphap_lin*(h*wp/2)*Bo+((wp/ws)*(gR_eff)*Psf)*(2*Ppf*(h*
wp/2)*Bo)^(1/2);

end

function dpbdz = g(z,b)

dpbdz = zeros(4,1);

%Parameters

ws = 193.3e12;
```

```
    wp = 206.5e12;

    if rf < 1
    alphas = 0.19/1000; %dB/m
    else
    alphas = 0;
    end

    alphap = 0.24/1000; %dB/m

    alphas_lin = alphas/4.343;
    alphap_lin = alphap/4.343;

    gR_eff = 0.72/1000;
    Aeff = 80e-12;

    gR = gR_eff*Aeff;%gR_eff*Aeff;

    Psb = b(1,:);
    Ppb = b(2,:);
    Nsb = b(3,:);
    Npb = b(4,:);

    %Evaluate coupled equations

    dpbdz(1) = ((-alphas_lin*Psb+(gR/Aeff)*Ppb*Psb)); % Signal evolution
    dpbdz(2) = ((alphap_lin)*Ppb + (wp/ws)*(gR/Aeff)*Psb*Ppb); % Pump evolution
    dpbdz(3) = (-
alphas_lin*Nsb+(gR_eff)*Ppb*Nsb)+(gR_eff)*((2*Ppb*Npb)^(1/2))*Psb+(alphas_lin+(gR_eff)*Ppb)*(h*ws
/2)*Bo;
    dpbdz(4) = -alphap_lin*Npb-
((wp/ws)*(gR_eff)*Psb)*(2*Ppb*Npb)^(1/2)+alphap_lin*(h*wp/2)*Bo+((wp/ws)*(gR_eff)*Psb)*(2*Ppb*(h*
wp/2)*Bo)^(1/2);

    end
    L = nz*dz; %Length of fiber
        Pf = 0.165; % Power launched in forward direction
        Pb = 0.165; % Power launched in backward direction
        Pin = Pf+Pb; % Total Power Launched
        Pso = 0.0001; % Initial input signal power
        rf = Pf/Pin; % Percentage of Raman gain in forward direction
         Pno = 0.000001; %-30dBm

    alphap = 0.24/1000;
    alphap_lin = alphap/4.343;
    Bo = 12.5e9; % Optical Bandwidth
    h = 6.626068e-34; % plancs constant

    zspan = linspace(0,L,nz+1);        %80km

    p0 = [Pso;
          Pin*(rf)
```

```
      Pno
      Pno];    %0dBm signal; 500mW pump

b0 = [Pso;
      Pin*(1-rf)*exp(-alphap_lin*L)
      Pno
      Pno];

[z,p] = ode45(@f,zspan,p0);
[z,b] = ode45(@g,zspan,b0);

%%%%%%%%%% Passive Fiber: NO RAMAN %%%%%%%%%%%%%
alphas = 0.19/1000;
grad = -alphas.*z;
%%%%%%%%%%%%%%%%%%%%%%%%%%%%%%%%%%%%%%%%%%%%%%%%

if rf == 0 || rf == 1;
    a = 10*log10(p(:,1)/Pso)+10*log10(b(:,1)/Pso);
else
    a = 10*log10(p(:,1)/Pso)+10*log10(b(:,1)/Pso)-(-alphas.*z);
end

gain = a-grad;


end
```

8.4 Gaussian Pulse

```
function u0 = gaussian(t,t0,FWHM,P0,m,C)

% This function computes a gaussian pulse with the specified
% parameters.
%
% USAGE:

%u = gaussian (t);
%u = gaussian (t,t0);
%u = gaussian (t,t0,FWHM);
%u = gaussian (t,t0,FWHM,P0);
%u = gaussian (t,t0,FWHM,P0,m);
%u = gaussian (t,t0,FWHM,P0,m,C);

% INPUT:

% t - vector of times at which to compute u
% t0 - center of pulse (default = 0)
% FWHM - full-width at half-intensity of pulse (default = 1)
% P0 - peak intensity (|u|^2 at t=t0) of pulse (default = 1)
% m - Gaussian order (default = 1)
% C - chirp parameter (default = 0)
```

```
%
% OUTPUT:
%
% u - vector of the same size as t, representing pulse amplitude

if (nargin<6)
  C = 0;
end
if (nargin<5)
  m = 1;
end
if (nargin<4)
  P0 = 1;
end
if (nargin<3)
  FWHM = 25;
end
if (nargin<2)
  t0 = 0;
end

u0 = sqrt(P0)*pow2(-((1+i*C)/2)*(2*(t-t0)/FWHM).^(2*m));
```

8.5 Histogram_samples_Q.m

```
close all; clear Q_samples;

delay_time_Tx_Rx = delay_time_Tx_Rx(length(delay_time_Tx_Rx));
% Q_samples = demodsignals(delay_time_Tx_Rx+1:length(demodsignals));

Gaussfilter_delay = 8;

Q_samples = clock_samples(delay_time_Tx_Rx+Gaussfilter_delay:length(clock_samples));

min_V = min(Q_samples);
max_V = max(Q_samples);
step_V = (max_V-min_V)/length(Q_samples);

Vthreshold = min_V:step_V:max_V;
figure(1);
grid on;
hist(Q_samples,Vthreshold);
```